

Stress and Deformation during Induction Hardening of Tubular Products

B. Lynn Ferguson, Z. (Charlie) Li
Deformation Control Technology, Inc., Cleveland, OH, USA
lynn.ferguson@deformationcontrol.com

Valentin Nemkov, Robert Goldstein
Fluxtrol, Inc., Auburn Hills, MI, USA

Key words: induction hardening, process modeling, residual stress, phase transformations

Abstract

Simulation of stresses and deformation during induction hardening is complicated. This paper is a follow on modeling work of induction hardening process presented at 26th HTS in Cincinnati, in October 2011 and UIE Congress in St. Petersburg, Russia, in May 2012. The previous studies were devoted to stress and deformation evolution during a single shot and scan induction hardening process, and the current paper focuses on comparison of these cases and on the methods of stress control in hardening of tubular products. Software ELTA is used to calculate the power and temperature distributions in terms of time from the induction heating process. The power distribution as a function of heating time is imported into DANTE to drive the model. The modeling results include the temperature distribution, phase transformations, stress state and deformation. The detailed coupling procedure between electromagnetic, thermal, stress and deformation phenomena during induction tube hardening is described.

The coupled modeling studies allow us to analyze effect of basic process parameters on the formation of stresses and deformation, which make it possible to optimize the process to reduce the cracking possibility, obtain specific microstructure and favorable residual stress state.

Introduction

Case hardening by induction heating followed by spray quenching is a well established method of surface hardening and also generating residual surface compression in outer diameters of shafts, both solid and hollow. However, cracking can be an issue, especially for bore hardening. A study was initiated to examine the differences between outer and inner surface hardening by induction using modeling. The first report from this study modeled a single shot process for a relatively thick walled tube [1]. Indeed, the outer surface was left under residual compression after hardening, while the bore surface was left under residual compression near the tube ends and residual tension over much of the bore length. A second report examined the effects of scanning hardening on the same tube geometries [2]. The results were similar, with scan hardening of the tube outer surface producing residual compression, and scan hardening of the tube bore producing a similar pattern of residual compression near the tube ends and residual tension over much of the length of the bore. This paper takes a more in depth look at the differences between outer and inner surface hardening and the reasons for these differences.

Modeling the Induction Hardening Process

Heat treatment of steel is complicated because of the phase transformations that must take place to accomplish hardening. Associated with these phase transformations are volumetric changes that are in the opposite direction of thermal expansion and contraction. For example, during heating the starting microstructure expands (normal thermal expansion), but as austenite forms, there is a volume contraction or shrinkage. As the austenitic material further heats, there is again expansion. During quenching, the situation is reversed, with the cooling austenite contracting initially. As the austenite transforms to martensite, there is volumetric expansion. Continued cooling of the newly formed martensite again results in dimensional contraction. The changes in dimensional growth and shrinkage generate considerable stress in the part, especially for induction hardening where only a portion of the part is heated and quenched and the changes in temperature are rapid. Stress is generated from the thermal gradients, the transformation strains, and the dimensional changes.

For induction hardening, there is an additional complication in that heating occurs in only a fraction of the part. The bulk of the part effectively anchors the overall shape and provides a heat sink. Electromagnetic, thermal and metallurgical phenomena interact to affect the local stress state and dimensional changes. Stresses appear from the very beginning of heating due primarily to thermal expansion of the surface layer. Electrodynamical forces created by electromagnetic field on the part surface are usually small compared to thermal and structural, and may be neglected. Exceptions to this include induction heating flat surfaces or thin, long parts.

Simulation Programs

Computer simulation of electromagnetic and thermal analysis has become an accepted tool for induction system design and optimization, and many commercial software packages are available. Fluxtrol, Inc. uses several programs, from the relatively simple Elta [3] to the more complex Flux 2D/3D Finite-Element package [4]. In combination with a structural analysis program such as DANTE, computer simulation offers a cost expensive method for tool and process development. The accuracy of simulation and completeness of the predicted information has introduced the phrase for this development procedure, “Virtual Prototyping of Induction Heat Treating” [5].

In this study the induction heating software Elta was used for electromagnetic and thermal simulation and the DANTE[®] [6, 7] package was used for thermal, structural, stress and distortion simulation. DANTE is a set of subroutines that add metallurgical modeling capability to the ABAQUS/STANDARD finite element software. The DANTE subroutines mathematically describe the mechanical, thermal and metallurgical phase transformations that occur during heating and quenching of steel components so that phase fractions, hardness, dimensional change and residual stress can be predicted throughout the thermal treatment. DANTE includes a database of steel alloys that covers the common carburizing and through-hardening grades of steel. It also includes data for surface heat transfer coefficients for more commonly used quenchants and quenching methods. However, DANTE does not have electromagnetic modeling capability, so it must be used in combination with such a program in order to simulate a process that relies on induction heating. References [6, 7] contain more detailed information on DANTE.

Elta is a program for electro-thermal simulation of induction heating processes. It is based on 1D finite difference method with analytical account for the length of the system. Elta is used to assess the effects of power, frequency and spacing between finite lengths of the part and

induction coil. Elta has a database for electromagnetic and thermal properties of different materials and temperature-dependent heat transfer coefficients for a variety of quenchants. There is also a capability to model progressive (scan) induction heating.

Figure 1 shows the calculations that are performed first by Elta, and then by DANTE. Elta calculates temperature histories and the induced power density distribution in the workpiece from the induction process variables that are entered by the user. The power density profile is passed into DANTE, and the temperature history for heating is recalculated, this time with austenite formation. During the spray quenching, the cooling history is calculated, as well as austenite decomposition to martensite and bainite. From the thermal and microstructural changes, the internal stress state and dimensional changes are calculated.

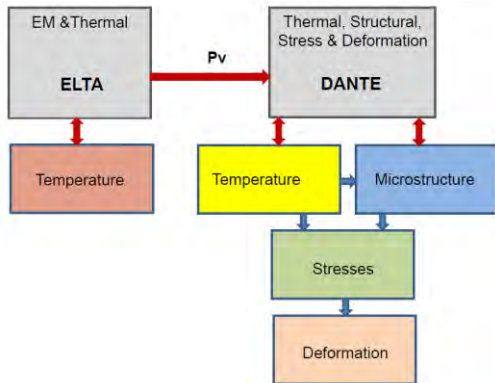


Figure 1 Calculations performed by Elta and DANTE and passing of data between the programs.

Case Study

OD and ID induction hardening of a thick walled tube was selected to study. A 4340 steel tube with an outer diameter of 0.28 m, inner diameter of 0.16 m and a length of 0.16 m was heat treated by the scanning process using an induction coil with the length of 0.025 m moving along the outer or inner surfaces. The heating and quenching processes were designed using Elta. The goal was to produce a case depth of about 6-7 mm while not exceeding a maximum surface temperature of 1100°C. Optimal frequency for this hardness depth is in a range of 1-3 kHz and a frequency of 2 kHz was chosen. Calculations showed that the required heating time should be about 18 seconds which corresponds to a scanning speed of 0.00139 m/s. Simulation showed that under these conditions the thickness of the hardened case, which corresponds to a temperature of approximately 800 °C during heating, would be 6 mm for ID heating and 6.8 mm for OD heating.

The spray quench was a water – 12% polymer solution. The spray head was attached to the bottom of the inductor, with a 45 degree spray angle and 0.050 m of spray coverage.

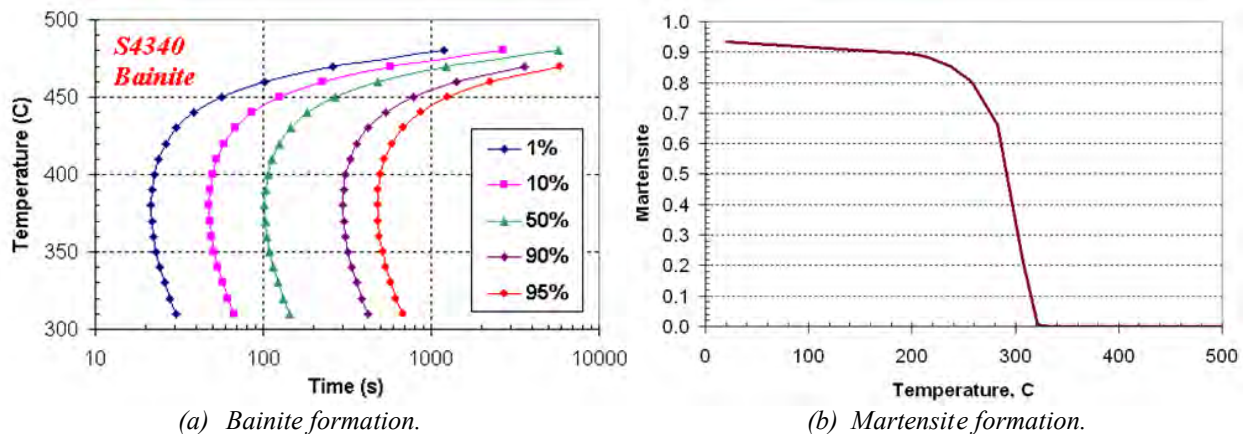
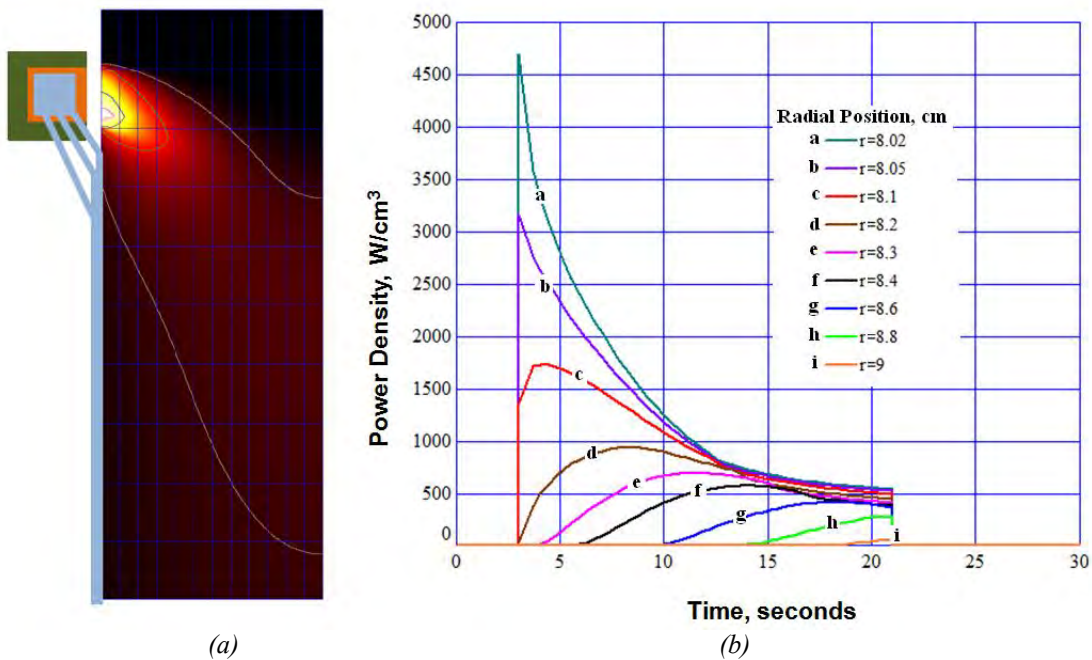


Figure 2 Kinetics data for 4340 steel.

The transformation characteristics of 4340 steel are shown in Figure 2(a) for bainite formation and (b) for martensite formation. The isothermal transformation curves for bainite formation in 2(a) and the continuous cooling curve for martensite formation in 2(b) were generated from the DANTE database parameters for 4340 steel.

Induction Scan Hardening of Internal Surface

Hardening the inner surface of the tube by induction scanning is presented first. A schematic of the tube ID scan hardening set-up and the internal temperature distribution is shown in Figure 3(a). Figure 3(b) shows the temperature profile predicted by the Elta software. The power distribution predicted by Elta was used by the DANTE model to predict the temperature development during scanning, and from this stress, displacement, phase transformation and final hardness calculations were made.



(a) Schematic of induction hardening and spray quench.
 (b) Elta predictions for power density distribution for tube ID heating.

A temperature contour plot at about the middle of the ID scanning cycle is displayed in Figure 4, along with the corresponding hoop stress and martensite distributions. A large layer of compressive stress appears above and outside of the formed austenite. This compressive zone moves upward ahead of the hot zone as scanning takes place. Outward of the newly formed martensite layer is a zone of high tensile hoop stress.

The temperature, martensite and hoop stress distributions are shown in Figure 5 at a scan time of 116 s which is just prior to the hot zone reaching the top of the tube. The large internal compressive stress zone has reached the top ID corner. The hoop stress at the bottom ID corner has become compressive, but the hoop stress in the martensite at mid-height is tensile, with a high tensile stress being present just below the hardened case.

The final stress distributions after ID quenching and cooling are displayed in Figure 6. A layer of tensile hoop stress is present over the mid-section of the tube ID to roughly the case depth. The hoop stress at the bottom and top ID sections is compressive. The axial stress on the

ID is compressive, except at the tube ends where it is zero. Both hoop and axial stresses are distributed along the tube non-uniformly. Figure 6 shows that the martensite thickness is increased at the top corner of the ID, and it is thinner at the bottom of the bore.

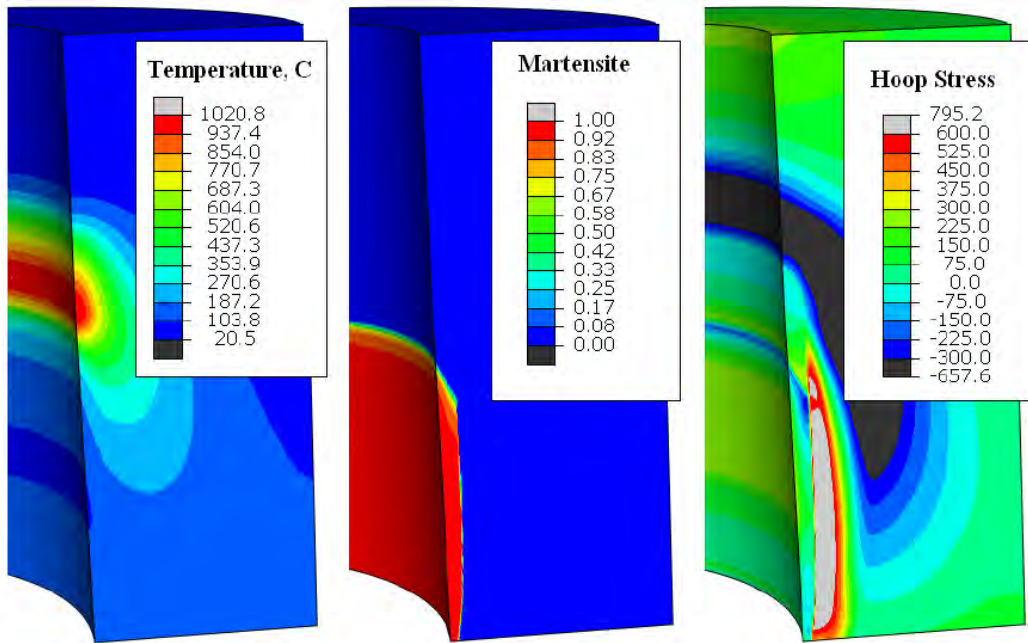


Figure 4 Temperature, martensite and hoop stress profiles predicted by DANTE at roughly midway through the ID scan hardening process. (Stress is MPa)

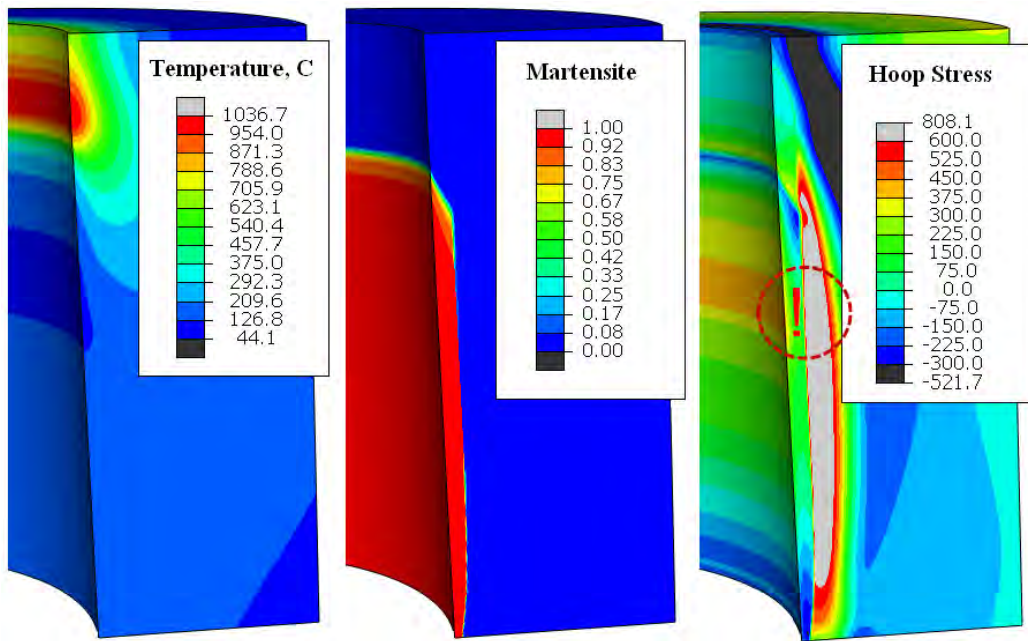


Figure 5 Temperature, martensite and hoop stress profiles predicted by DANTE nearing completion of the process. (Stress is MPa)

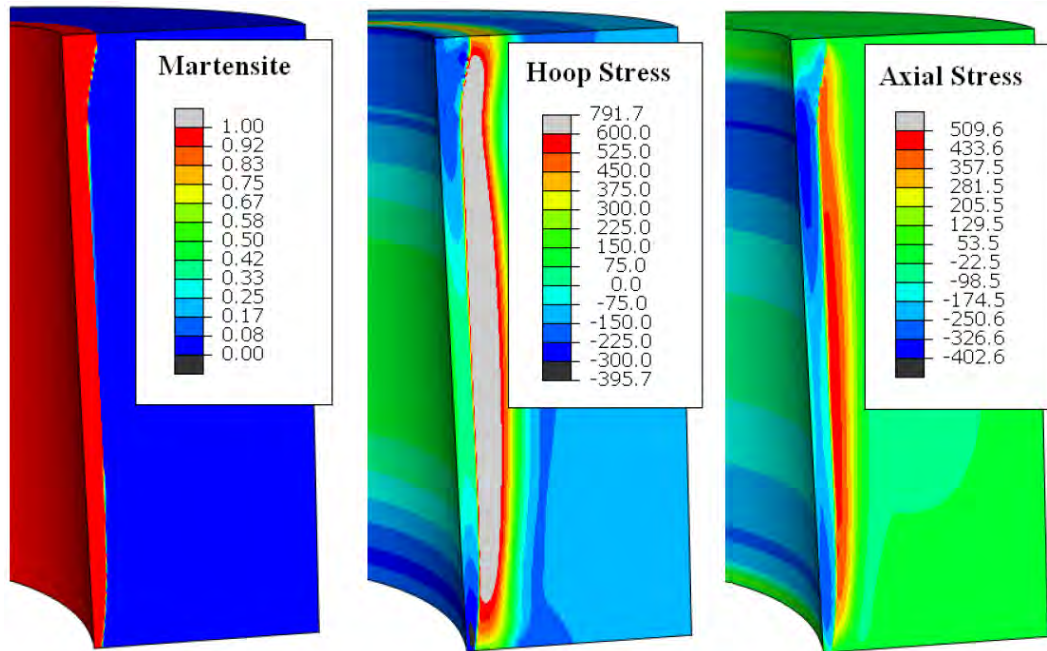


Figure 6 Final martensite, hoop and axial stress profiles predicted by DANTE. (Stress is MPa)

The compressive axial stress layer and the tensile hoop stress at mid-height on the bore of the tube are immediately backed by a layer of significant tensile stresses at depths from 7 to 15 mm. The remainder of the body maintains a slight state of hoop compression and mild axial tension. The hoop stress pattern at the ends of the tube is termed “Stress End Effect of the Part” as this is a common occurrence.

Figure 7 shows temperature, austenite formation and decomposition to martensite, and hoop stress histories at mid-height of the bore of the tube throughout the ID scanning process. After about 50 seconds this location begins to heat and the region transitions into deep compression (-700 MPa) as thermal expansion of the heating layer is restricted by the underlying cold substrate. As austenite forms, the compression is relieved due to the BCC to FCC crystal structure change. The austenite is then stretched in tension by neighboring and underlying material expansion. During spray quenching, martensite formation quickly imposes hoop compression, but neighbor and subsurface constraints reinstitute tensile stress. This bore location remains in hoop tension of about 100 MPa after process completion. As will be shown, this is considerably different than the stress state produced by OD scan hardening.

Induction Hardening of Tube Outer Surface

Scan hardening of the outer surface model results are reported in this section. Similar to the ID hardening section, results are shown for a mid-process, near the end of the heating step and after completion of the process. Figure 8 shows through-thickness views of temperature, martensite fraction and hoop stress predicted for mid-process. Martensite has formed in the lower half of the tube outer wall. The peak wall temperature of 1112° C is on the outer surface. The temperature profile has penetrated into the part by diffusion, but because of the upward scanning motion, the profile angles downward into the tube section. The martensite layer is in compression, but there is fairly strong tension in the adjacent material. A strong compressive

zone is advancing ahead of the hot zone. As the heating period is nearly completed, Figure 9 shows that the compressive stress zone has moved to the top of the tube, and the tensile zone under the martensitic layer has remained and grown with the martensite. The martensite itself is under a mix of tensile and compressive stresses. After completion of the OD scan hardening process, Figure 10 shows that the martensite layer is thicker at the top corner and thinner at the bottom OD corner, just as for the ID scan hardening case. There is a fairly strong tensile stress zone inside of the martensitic layer; again, this is similar to the ID hardening response in Figure 5. The big difference between OD and ID hardening shows up when looking at the stress in the hardened layer. In Figure 9 for OD scan hardening, the hoop and axial stresses are compressive in the martensite. Recall from Figure 6 that ID hardening was predicted to produce residual tensile stress at mid-height in the martensite layer.

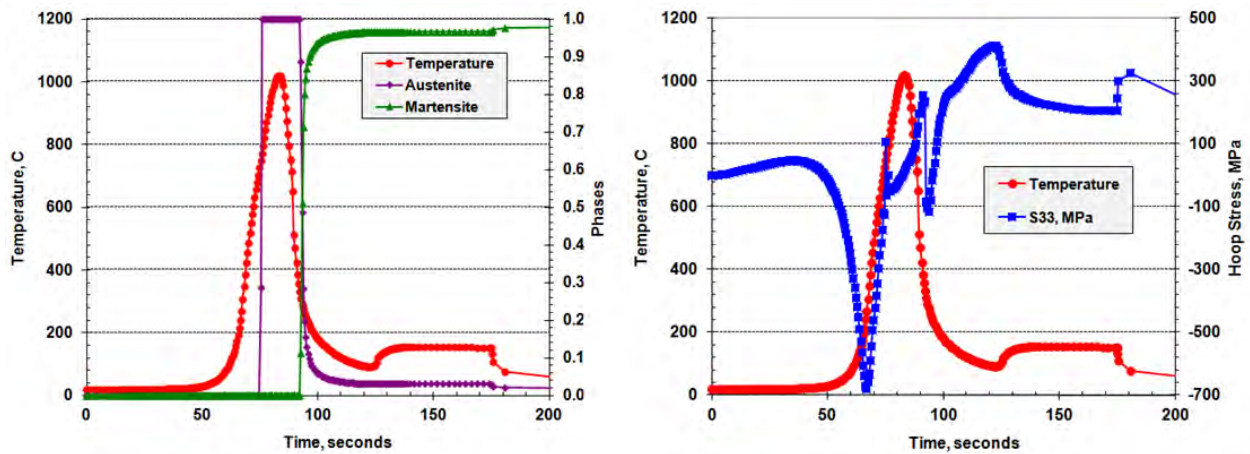


Figure 7 Temperature, phase and hoop stress histories experienced at the mid-length bore location of the tube. (N.B. Process is not completed until 475 seconds.)

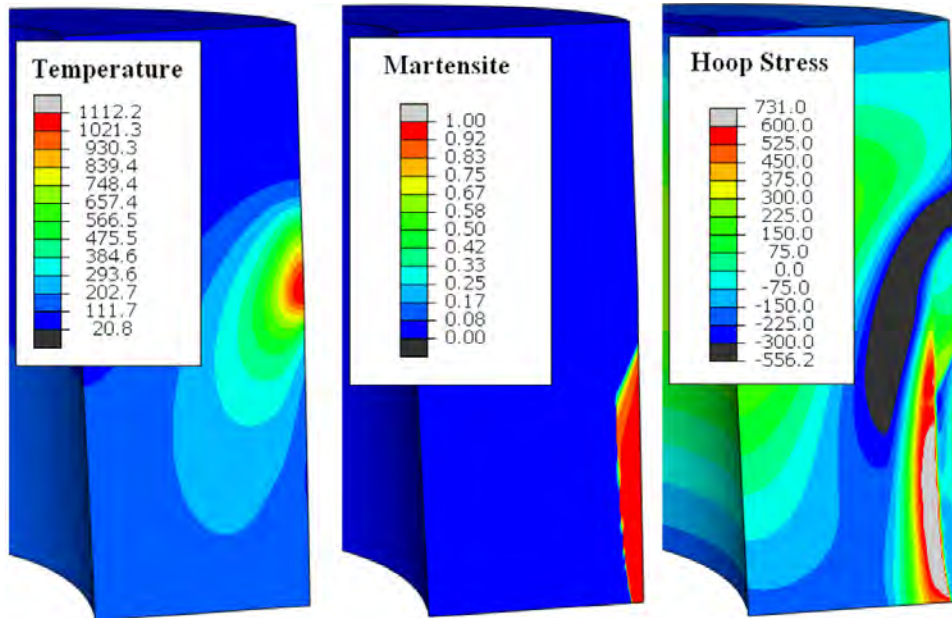


Figure 8 Predicted temperature, martensite and hoop stress profiles at roughly midway through the OD scan hardening process. (Stress is MPa)

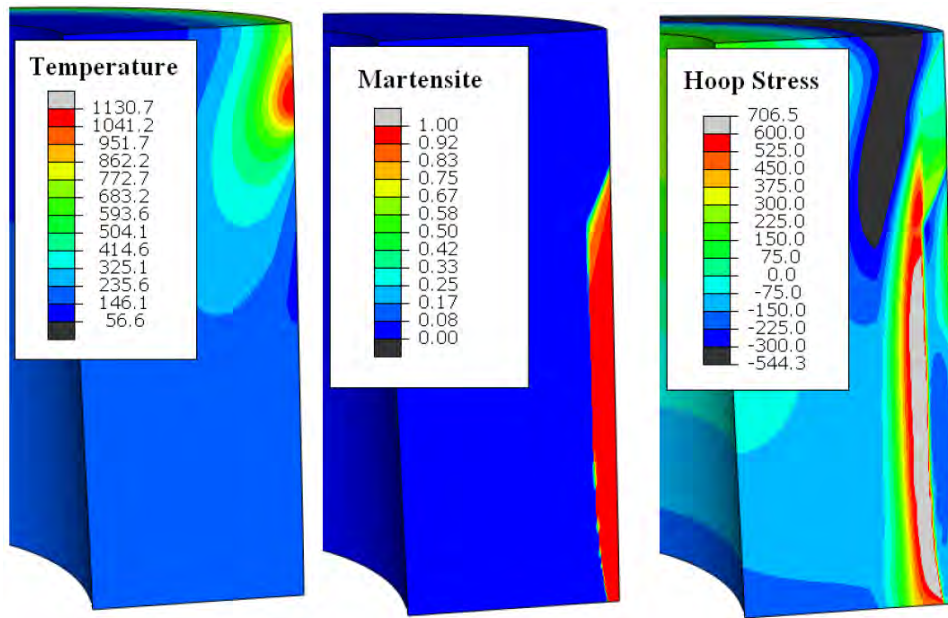


Figure 9 Temperature, martensite and hoop stress profiles predicted near completion of the heating step of the scan hardening process. (Stress is MPa)

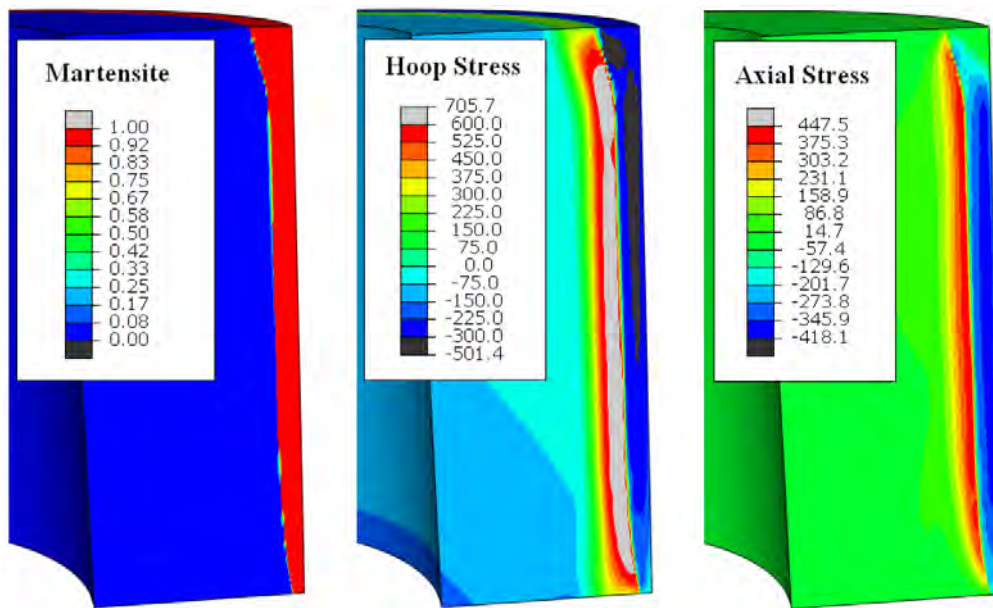


Figure 10 Final martensite, hoop and axial stress profile predictions for OD scan hardening.

Figure 11 shows the temperature, phase and hoop stress changes with time during the scan hardening process at mid-height on the OD surface. This is similar to the history plots in Figure 7 for ID hardening. The mid-height location enters under the inductor face at the 52nd second after the beginning of the process and temperature rises quickly up to approximately

1100° C during the 18-second heating time. Austenite forms quickly as the temperature rises above the upper critical temperature, A_{c3} . As the inductor leaves this location, the temperature starts to fall due to heat soaking for 3.2 seconds before the surface point enters into the spray quenching zone. Conversion of austenite to martensite starts when the surface temperature drops below M_s point (about 350°C). As a result the fraction of austenite quickly drops with corresponding growth of the martensite fraction. After 10 seconds of quenching the surface enters in a low intensity cooling zone, after which the final water cooling takes place.

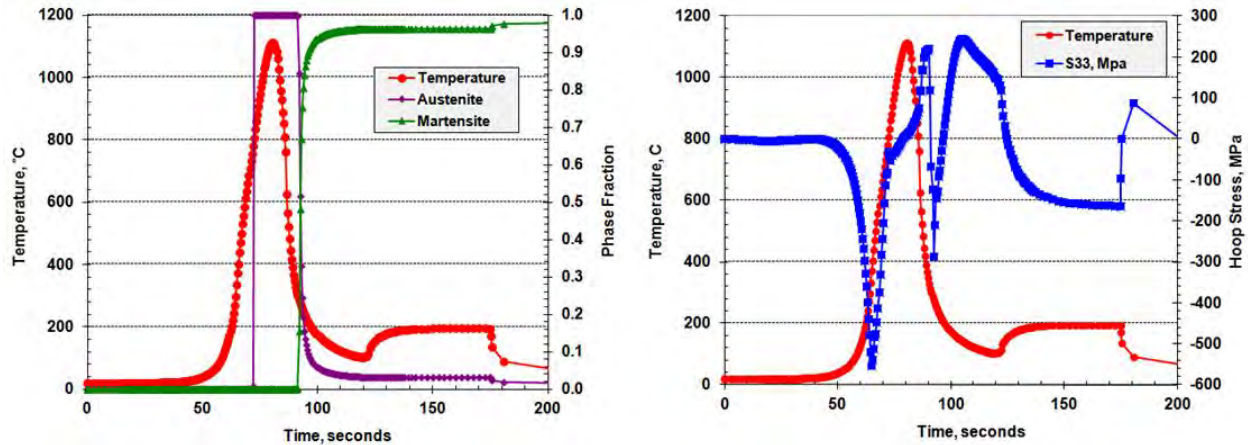


Figure 11 Temperature, phase and hoop stress histories experienced at the mid-length bore location of the tube. (N.B. Process is not completed until 475 seconds.)

Discussions

For both ID and OD scan hardening, the thinner layer of martensite at the start of hardening is due to the influence of axial heat transfer because of slow scanning speed. This non-uniformity may be easily corrected by power and scanning speed variation at the beginning of heating. Similarly, the thicker layer of martensite at the top of the tube and end of scan heating is due to heat accumulation by means of diffusion in the axial direction. This also can be easily corrected by process adjustments.

It is important to understand stress evolution during heat treatment, especially on the part surface where tendency for cracking is highest. For ID hardening, Figure 7 shows that the rapid heating generated a bore surface stress of -700 MPa that quickly changed to a tensile stress of +100 MPa as the subsurface temperature increased. As austenite formed on the surface, the stress became compressive at -100, but quickly rose to a tensile stress of +250 MPa as austenite and heating occurred beneath the surface. Martensite formation during quenching drove the surface stress into compression of about -100 MPa, but as martensite formed beneath the surface, the surface stress rose to about +450 MPa. Cooling and final thermal contraction only dropped the surface stress to about +100 MPa. While martensite should be able to withstand a stress of +450 MPa, a surface flaw or defect or more complex geometry of the part could easily generate a locally higher stress and result in cracking. At best, the final residual tensile stress on the ID is detrimental to part performance.

Figure 11 shows variation of temperature and hoop stresses on the OD surface in the middle cross-section of the parts. Rapid surface heating causes strong compressive stresses which reach -550 MPa. These stresses dissipate as the surface layer gets hot, and then become tensile (up to 200 MPa) in the process of austenite cooling before formation of martensite, which results in fast reversal of stress to compression. Penetration of a phase transformation front into

the depth and thermal expansion of the rigid internal layers below the austenite layer due to further heat soaking cause the surface stress to again become tensile (the second peak in a positive range). Further variations of surface stresses are due to the overall temperature distribution in the part wall. Residual stresses on the OD surface are compressive (close to -280 MPa), which is a positive factor for the part operation in service. For OD scan hardening, the highest surface stress was about half that of ID hardening, and cracking is much less of an issue.

Dimensional Changes: Comparing Scanning and Single Shot Hardening

Figure 12 shows cross sectional comparisons of the predicted radial displacements for both OD and ID hardening using the single shot method and the scanning method. Parts (a) and (b) are for OD hardening, and parts (c) and (d) are for ID hardening. Parts (a) and (c) are for scan hardening, and (b) and (d) are for single shot hardening. The dimensional changes in these figures have been magnified twenty times so it is easier to identify the shape distortion. For OD hardening, the tube shrinks radially for both single shot and scan hardening as shown in Figures 12 (a) and (b). This makes sense in that the OD hoop stress for both cases is compressive. Single shot hardening of the OD surface, Figure 12 (b), produces dimensional change that is symmetric bottom to top while it isn't symmetric for scanning. Comparison of the contour patterns and the OD corner feature bears this out. The OD surface for single shot bulges more than the scan hardened OD surface, and actually is predicted to grow about 7 microns while the tube body shrinks.

For tube ID hardening, both the bore and the OD are predicted to shrink in comparison to the starting dimensions, see Figure 12 (c) and (d). For single shot hardening, part (d), the radial shrinkage of the bore is predicted to be -0.146 mm and for the outer wall it is -0.058 mm. The most significant shrinkage is predicted at mid-height of the tube ID, and this is approximately two times the radial shrinkage at the tube ends. This is also true for ID scan hardening. As for OD hardening, single shot ID hardening produces symmetric dimensional change while the scan hardening does not. The ID corner geometries for scan hardening are different, as shown.

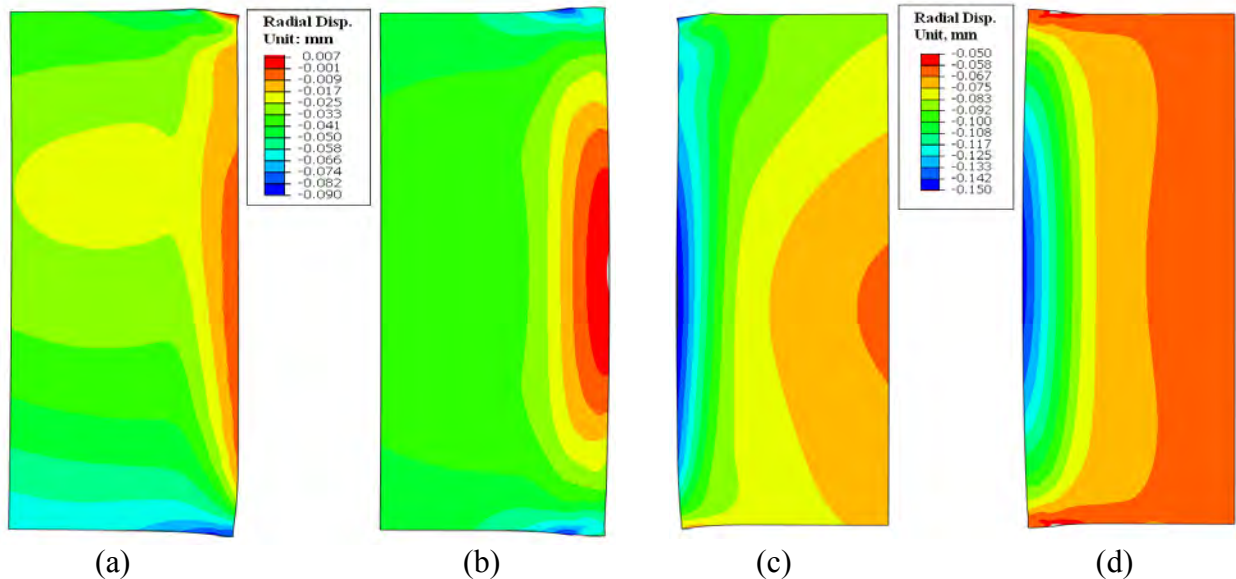


Figure 12 Radial displacement distribution at the end of cooling for OD and ID treatment.

(a) and (c) – scan hardening; (b) and (d) – single-shot hardening (Dimensional changes are magnified 20X)

Conclusions

Internal stresses due to temperature variation and structural transformation during induction processing may be positive (shrink-fitting, bending strength improvement) or detrimental/negative (deformations, cracks, service properties reduction). In order to achieve the desired final properties of a material, the phenomena that occurs during the cycle needs to be understood and predictable. Residual stresses and part deformation after induction surface hardening depend upon many factors: part geometry, alloy chemistry and initial microstructure of the material, case depth, heating and quenching parameters. It is very difficult or even impossible to predict the interaction of all these factors by empirical methods alone. Because of the many stress reversals that accompany hardening, intuition is easily fooled. Computer simulation is a powerful tool for analysis of stresses and deformation evolution during the entire processing cycle.

This study of a thick-wall tube induction treatment using the Elta and DANTE programs showed that the final stress distribution is different for ID and OD surface hardening. Hoop stress distribution along the part length is not uniform with hoop stress concentration near the tube ends for ID hardening and in the central zone for OD hardening. Dimensional distortion of the part may be significant during the treatment process even if the final deformation is small.

Stress evolution shows a reversal behavior with a possibility of high tensile stresses during the martensite formation, which can lead to quenching cracks. This effect is stronger for ID hardening than for OD hardening.

Computer simulation can predict stress and deformation evolution and provides a means for finding scenarios for control and optimization of heat treating and following surface finishing processes with an account for residual stresses. Interdisciplinary collaboration is important for better understanding of evolution of stresses and distortions during induction heat treatment and improvement of tools for their prediction.

References

- [1] V. Nemkov, R. Goldstein, J. Jackowski, L. Ferguson, Z. Li, "Stress and Distortion Evolution During Induction Case Hardening of Tube," ASMI-HTS 2011 Conference Proceedings, Cincinnati, OH, October, 2011.
- [2] V. Nemkov, R. Goldstein, L. Ferguson, Z. Li, "Stresses and Distortions During Scan Induction Case Hardening of Thick Tube," UIE Congress, St. Petersburg, Russia, May, 2012.
- [3] Elta (www.nsgsoft.com)
- [4] Flux 2D/3D (www.magsoft-flux.com)
- [5] Z. Li, A. Freborg, B. Ferguson, Application of modeling to heat treat processes. Heat Treating Processes, May/June 2008.
- [6] D. Bammann, et al., "Development of a Carburizing and Quenching Simulation Tool: A Material Model for Carburizing Steels Undergoing Phase Transformations," 2nd Int. Conference on Quenching and Control of Distortion, ASM Int., 1996.
- [7] R. Goldstein, V. Nemkov, J. Jackowski, "Virtual Prototyping of Induction Heat Treating," Proc. of the 25th ASM Heat Treating Society Conference, Indianapolis, Sept. 14–17, 2009.